Algal Research 71 (2023) 103091

Contents lists available at ScienceDirect

Algal Research

journal homepage: www.elsevier.com/locate/algal

Utilizing lipidomics and fatty acid synthase inhibitors to explore lipid accumulation in two thraustochytrid species

E-Ming Rau [a], Inga Marie Aasen [b], Zdenka Bartosova [a], Per Bruheim [a], Helga Ertesvåg [a,*]

[a] Department of Biotechnology and Food Science, NTNU Norwegian University of Science and Technology, Trondheim, Norway
[b] Department of Biotechnology and Nanomedicine, SINTEF Industry, Trondheim, Norway

ARTICLE INFO

Keywords:
Thraustochytrids
Aurantiochytrium
Docosahexaenoic acid
Lipidomics
Fatty acids
FAS inhibitor

ABSTRACT

Thraustochytrids are marine protists with an excellent ability to produce health-beneficial docosahexaenoic acid (DHA)-rich lipids. Since the demand for DHA sources for food and feed is increasing, a deeper understanding of the potential to enhance the DHA-production in thraustochytrids is important for a sustainable DHA supply. In most thraustochytrids, including the strains used in this work, DHA is synthesized by a polyketide synthase-like pathway (PKS), and not through the common fatty acid synthetase (FAS) pathway. Both pathways use the same precursors. The aim of this study was to determine if inhibiting the production of fatty acids (FA) through the FAS pathway under nitrogen starvation would result in higher net DHA production rates measured as DHA content, and if the channeling of the synthesized fatty acids to different lipids species is similar in two different thraustochytrid strains. We found that the DHA production rates in *Aurantiochytrium limacinum* SR21 and *Aurantiochytrium* sp. T66 were not affected when treated with the FAS-inhibitor cerulenin, despite a reduction of FAS-derived FAs. This indicates that precursor availability is less likely to be the limiting factor for DHA synthesis. Still, cerulenin-treatment in the lipid accumulation phase resulted in higher concentrations of the triacylglycerol (TAG) TG(22:6/22:6/22:6) than in the untreated cells after three hours, demonstrating that FAS inhibition is a possible strategy to enhance the content of DHA-rich lipids. Moreover, the relatively high abundance of the diacylglycerol DG(22:6/22:6) suggests the presence of an obstacle for using DG(22:6/22:6) as substrate to synthesize DHA-rich TAGs, a step that potentially can be improved by metabolic engineering.

1. Introduction

Docosahexaenoic acid (DHA) is an essential ω3 polyunsaturated fatty acid (PUFA), and since the demand for DHA for food and feed is increasing, sustainable DHA sources are becoming increasingly more important with a high potential for market growth [1]. Thraustochytrids are marine protists that can produce and store DHA-rich lipids and are already used for commercial DHA production [2–4]. Still, in order to be economically competitive for low-cost products like fish feed, there is a need to improve the production of DHA by thraustochytrids.

Thraustochytrids store triacylglycerols when a carbon source is available and their growth is stalled by limited supply of another essential nutrient, typically nitrogen. In thraustochytrids, saturated fatty acids (FAs) are synthesized by the fatty acid synthase (FAS), while two pathways synthesize unsaturated FAs. The desaturase-elongase pathway synthesizes monounsaturated FAs (MUFAs) and some PUFAs, while DHA and DPA (docosapentaenoic acid) are synthesized by a polyketide synthase-like (PKS) pathway in most studied thraustochytrids [5,6], although a *Parietichytrium* sp. recently were shown to use the desaturase-elongation pathway [7].

One strategy to enhance the production of a targeted pathway is to reduce or remove the flux of competing pathways [8]. Since both PKS and FAS pathways use the same precursors, acetyl-CoA and NADPH, inhibiting FAS could potentially channel more of these precursors towards the PKS pathway. One way to test this assumption, would be to inhibit the reactions catalyzed by FAS and measure if this enhances the DHA production rate. Several inhibitors can inhibit the FAS pathway, such as cerulenin, isoniazid and taxifolin [6,9,10]. It has been shown that in short-time labelling experiments, cerulenin inhibited FAS more efficiently than the PUFA synthase in both *Schizochytrium* sp. and *Thraustochytrium* sp. 26,185 [6,11]. Similarly, cerulenin treatment increased the proportion of DHA in total FA in *Aurantiochytrium mangrovei* BL10 and *Schizochytrium* sp. S056 when added during fermentations [12,13]. In all these studies, cells were treated with cerulenin in the

* Corresponding author at: Department of Biotechnology and Food Science, NTNU, N-7491 Trondheim, Norway.
E-mail address: helga.ertesvag@ntnu.no (H. Ertesvåg).

https://doi.org/10.1016/j.algal.2023.103091
Received 29 September 2022; Received in revised form 3 March 2023; Accepted 3 April 2023
Available online 5 April 2023

exponential growth phase, when phospholipid (PL) is the main lipid class produced [14]. It is not known how the DHA production is affected by inhibiting FAS during the N-depletion phase, when triacylglycerols (TAG)s are the dominating lipid class produced. An enrichment of DHA in the lipids could be advantageous, even without increased productivities, as the costs of separation and purification in the following downstream process for producing high-DHA content lipid products in industry would be reduced [15]. Still, whether FAS inhibition can be applied to facilitate the production of DHA-rich lipid species remains to be explored.

Lipid accumulation characteristics can be different among thraustochytrid species and strains. *Aurantiochytrium* sp. T66 (hereafter called T66) has a desaturase that generates a more diverse FA profile with two additional MUFAs (C16:1 and C18:1) not produced by *Aurantiochytrium limacinum* SR21 (hereafter called SR21) [16–18]. In this study, we characterized the lipid accumulation in T66 and SR21 after N-depletion. Both strains were treated with cerulenin as they entered the N-starvation phase, to examine the effect of FAS inhibition on DHA production rates. Moreover, in a previous work, we have characterized the lipid composition of T66 and the changes during fermentation by high-resolution MS [19]. Here we use the same methods to compare the lipid composition of the two strains, and to study how the FA composition of the lipid species is affected by the available FAs after cerulenin treatment.

2. Materials and methods

2.1. Cultivation conditions

For tests of the effects of the inhibitors, *Aurantiochytrium limacinum* SR21 (ATCC MYA-1381) and *Aurantiochytrium* sp. T66 (ATCC PRA-276) were cultivated in bioreactors. It should be noted that a phylogenetic study placed T66 in the novel genus *Hondea* [14]. A minimal medium with 70 g/l glucose as carbon source and NH_4Cl (2.0 g/l) as nitrogen source was applied [19]. The inoculation medium and all conditions were as described by Bartosova et al. [19] with the cultivation starting with 4 % *v*/v inoculum culture. The aeration rate was 0.3 vvm. The temperature was 25 °C. The CO_2-production rate was measured by a mass spectrometer (Balzers Omnistar GSD 300 02, Pfeiffer Vacuum GmbH, Germany), calculated based on the fermentation start volume. When nitrogen was exhausted in the cultures, as indicated by a drop in the CO_2-production rate (approx. 7 g/l dw), the cultures were transferred either to microbioreactors or shake flasks. For the microbioreactors, the cultures from the bioreactors were transferred to 48-well microplates (BioLector®, m2p-labs GmbH, Germany), 1 ml per well, prefilled with concentration series of the inhibitors, and incubated for 15 h at 800 rpm, with pH-control and logging of dissolved oxygen and the increase in biomass. The inhibitors were dissolved in ethanol (cerulenin), DMSO (taxifolin) or water (isoniazid). For the final growth experiment, the cultures from the bioreactors were transferred to 250 ml conical baffle flasks, 50 ml per flask, prefilled with concentration series of cerulenin (no cerulenin (= 0), 1, 5 and 25 μM), and incubated for 12 h at 170 rpm.

2.2. Fatty acid and glucose analysis

FA concentrations were determined by LC/MS/MS (QQQ) after hydrolyzing lipids directly from the culture samples to free FAs as previously described [20]. For measuring glucose concentration in culture medium, 1.5 ml culture was centrifuged at 4500 ×*g* (4 °C) for one minute. The supernatant was stored at −20 °C for later analysis. Just before analysis, samples were diluted five times by water and filtered (0.2 μm). The concentrations of glucose were then determined by HPLC [21].

2.3. Lipid extraction and total lipid content determination

1.5 ml of the culture was centrifuged at 4500 *g* for 1 min, followed by washing the cells with 3 ml mineral medium and then by 3 ml milli-Q water. Liquid nitrogen was used to snap-freeze the cell pellet for about 10 s before it was stored at −20 °C for later extraction.

Frozen cell pellets were lyophilized overnight. Zirconium oxide beads (0.5 ± 0.01 g, Ø 1.4 mm) were mixed with five milligrams of dried cell pellets in 2 ml vials, including a blank control without cells, before adding 1 ml of a cold mixture of chloroform:methanol (1:2, *v*/v). The mixtures were homogenized by a Precellys®24 bead homogenizer with a Cryolys temperature controller (all Bertin Technologies SAS, Montigny-le-Bretonneux, France) at 6500 rpm for 30 s plus 15 s intermediate pause, repeated three times. The homogenized cells were then mixed with 333 μl cold chloroform, followed by vortexing for 20 s, before addition of 333 μl of water and vortexing for 20 s to induce phase separation before the samples were centrifuged at 14000 rpm for 5 min at 15 °C. The lower chloroform layer containing the lipids was collected. Cell debris was cleared by a syringe filter with PTFE membrane, 0.2 μm, Ø 13 mm (VWR, USA). The extracts were flushed with a stream of nitrogen. The samples were stored at −80 °C in dark glass vials for total lipid content analysis and lipid species determination.

For measuring total lipid content, 300 μl of lipid extract was transferred to a pre-weighed glass vial, left in fume hood for evaporation and weighed after two days. The lipid content was then calculated by knowing that the chloroform phase was 666.3 μl.

2.4. Lipid classes and species analysis

Lipid extracts were analyzed by a nontarget semiquantitative lipidomics method based on ultrahigh performance supercritical fluid chromatography (UHPSFC)-mass spectrometry (MS) for determining lipid classes and species, as previously described [21]. Lipid species were tentatively identified based on mass accuracy (<5 ppm), the retention time of relevant lipid class, isotopic pattern and fragmentation pattern (if available) without distinguishing the specific sn positions of each fatty acyl group on the corresponding head groups. TG(52:6), TG(46:0), TG(58:12), TG(49:6), TG(44:0) and PC(40:7) were interpreted as TG(14:0/16:0/22:6), TG(14:0/16:0/16:0), TG(14:0/22:6/22:6), TG(14:0/14:0/22:6), TG(14:0/14:0/16:0) and PC(22:6/18:1) respectively, based on the result of FA composition analysis. The abundance was normalized by the default method in Progenesis QI software. The abundance of individual lipids was then multiplied by the estimated biomass (T66: 8 g/l at 3 h and 10 g/l at 12 h; SR21:8.1 g/l at 3 h and 12.5 g/l at 12 h) to be interpreted as relative concentrations. The differences in ionization efficiency of each lipid class were corrected by response factors, which were estimated experimentally as previously described [21].

2.5. Statistical analyses

For the quantitative analyses, three biological samples were used. Standard deviation was calculated using the formula $\mathrm{STDEV}=\sqrt{\sum (x-\bar{x})^2 / (n-1)}$. Unpaired t-tests were calculated using Graphpad (www.graphpad.com).

3. Results

3.1. Exploring the effect of different FAS inhibitors on the FA composition of cells

Firstly, three different FAS inhibitors were tested to identify a compound that inhibits FAS in both *Aurantiochytrium* species and does not inhibit the PUFA synthase to the same degree. Cerulenin can inhibit FAS

by binding the β-ketoacyl-ACP synthase (KS) domain of FAS [6]. Isoniazid can suppress FAS by inhibiting the enoyl reductase function of FAS [9]. Taxifolin is a flavonoid that can inhibit FAS by competing with acetyl-CoA for the same active site of FAS [10].

When using defined media, the fatty acid and lipid accumulation rates in T66 [19,20] and SR21 (unpublished) are high and constant the first 15–20 h after N-exhaustion, before they start to decrease. Thus, both strains were cultivated in bioreactors until reaching N-starvation, as indicated by no further increase in the CO_2-production rate, followed by transfer of the biomass to microbioreactors for treatment with taxifolin, isoniazid and cerulenin for 15 h. This allowed us to compare the effect of the inhibitors on otherwise identical cultures. A pre-study had been run to identify suitable concentrations of each inhibitor. This study suggested that T66 was more resistant to these inhibitors than SR21, hence different concentrations were used for the two strains. The cerulenin-treated cells showed lower concentrations of the FAS pathway-derived FA (FAS-FAs) than the control without inhibitors, while PKS-derived FA (PKS-FAs) or DHA remained at similar concentrations in both T66 and SR21 (Fig. 1a and d). The result is consistent with previous reports [12,13], showing that cerulenin can potentially inhibit FAS-FAs production in T66 and SR21 without affecting the level of PKS-FAs or DHA significantly under N-starvation. In both strains, addition of isoniazid had a similar effect on both FAS and DHA (Fig. 1b, e). Taxifolin seemed to slightly increase the production of FAS and DHA in SR21, while a small reduction of FAS was observed for T66 (Fig. 1c and f).

3.2. Fatty acid production rates and the effects of cerulenin during N-starvation

Based on these preliminary results, an experiment was set up to measure and compare the production of different FAs and lipids in the two strains and how they responded to cerulenin treatment. As before, T66 and SR21 were cultivated in bioreactors until reaching nitrogen starvation. The cultures were then aliquoted to shake flasks since the larger volumes would allow for sampling as a function of time. Different amounts of cerulenin, no (denoted 0 μM), 2, 5, and 25 μM, were added at time zero, this would allow us to observe any effect of increasing dosages. The cells were collected for analyses after 0, 3, 6, 9 and 12 h. The cell mass concentrations were approx. 7 g/l at transfer from bioreactors to shake flasks, and had reached 10 and 12.5 g/l, respectively for T66 and SR21 after 12 h.

The concentrations of the different FAs at the five time points were measured for each culture (Supplementary Fig. S1). From 0 to 12 h, the concentration of all the detected FAs increased. The cerulenin-treated SR21 had lower FAS-FA levels than the untreated cells after 3 h. SR21 accumulated almost no FAS-FA from 0 to 3 h when treated with 25 μM cerulenin, but after the first three hours, FAS-FA concentration increased at a similar rate regardless of the concentration of cerulenin (Fig. 2a and Table 1). For T66, the concentration change caused by cerulenin was smaller. Although not significant based on the standard deviations and t-test, an apparent trend indicating some inhibition of FAS was observed. In contrast, no effects of cerulenin were found on PKS-FAs or DHA accumulation rates in any of the two strains. The results showed that although FAS inhibition increased the proportion of DHA of total FA (Table 1, Supplementary Table S1 and Fig. S2), the concentration of DHA did not increase. The glucose consumption rates (Fig. 3a and b) correlated with the FA production rates, with a FA yield on glucose of approx. 22–25 % (Fig. 3c).

3.3. The production of total lipid of T66 and SR21 and how it was affected by cerulenin during N-starvation

Samples from 3 h and 12 h were selected for analysis of total lipid content and high-resolution lipid profiling. The 25 μM cerulenin-treated T66 and SR21 contained lower amounts of lipids than the untreated cells after 3 h (Fig. 4a). However, after the first three hours the lipids increased at a similar rate regardless of the concentration of cerulenin (Fig. 4b), showing that the effect of cerulenin did not persist for a long period.

3.4. The triacylglycerol species of T66 and SR21 and how they were affected by cerulenin during N-starvation

Thraustochytrids store lipids as neutral lipid triacylglycerol (TAG), and already after 3 h, TAG accounted for >70 % of the total lipids in both strains (Fig. 5a and b). Diacylglycerol (DAG) was the second most abundant lipid class on average of the two strains and the two time points, while phosphatidylcholine (PC) was the most abundant phospholipid class.

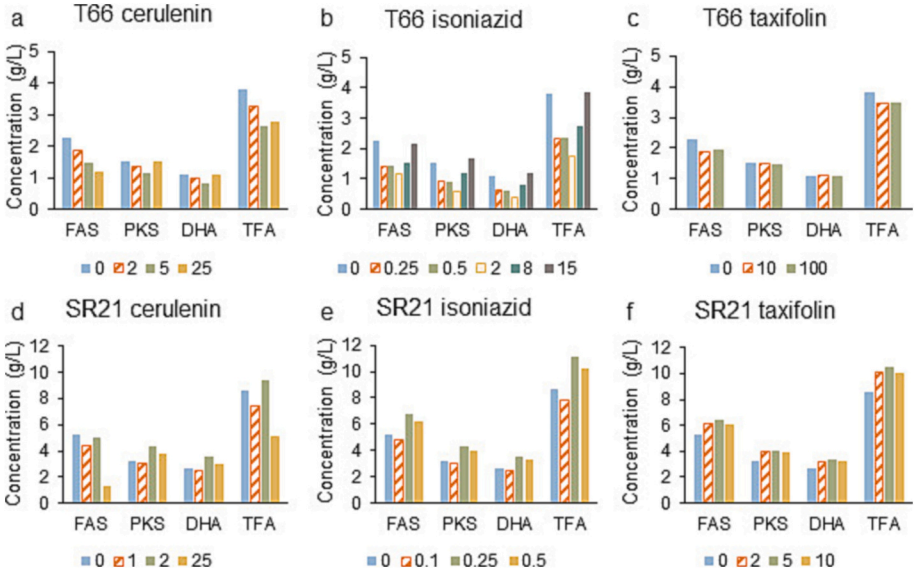

Fig. 1. Concentrations (g/l, y-axes) of fatty acids in T66 and SR21 after being treated with cerulenin (a, d), isoniazid (b, e) and taxifolin (c, f) for 15 h after N-starvation. Inhibitor concentrations (μM) are shown in the legends. FAS, the sum of C14:0, C16:0, C16:1 and C18:1; PKS, the sum of DHA and DPA; TFA, total fatty acids.

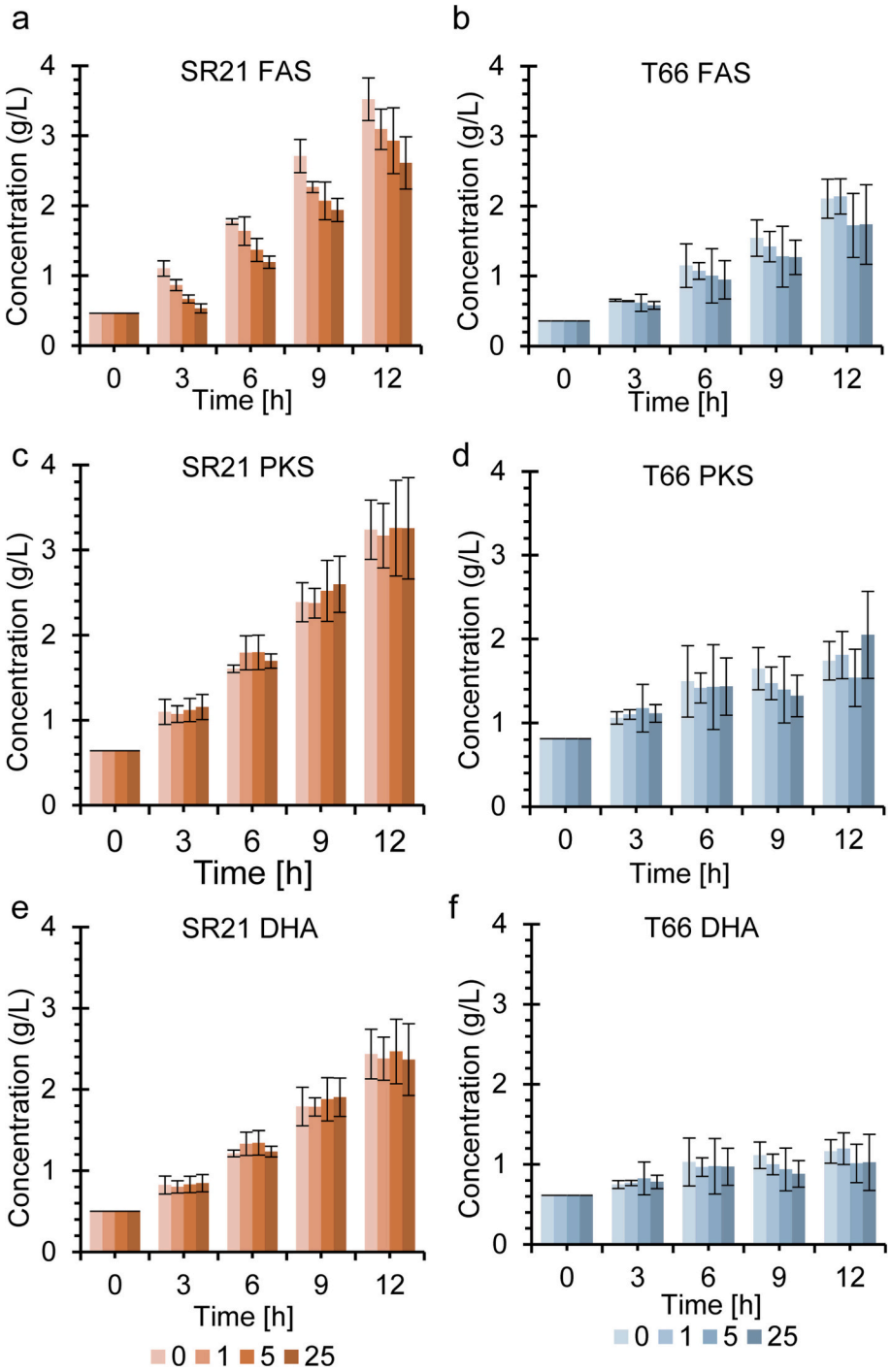

Fig. 2. Time-course profile for fatty acid concentrations in SR21 (a, c and e) and T66 (b, d and f) treated with cerulenin. Cerulenin concentrations (μM) are shown in the legends. FAS, the sum of C14:0, C16:0, C16:1 and C18:1. PKS, the sum of DHA and DPA; All data are expressed as the mean of three independent cultures, except data from 0 h, originating from one culture; Error bars represent the standard deviation. Data with '*', $p < 0.05$ by unpaired t-test vs. the value without cerulenin treatment at the same time point. Data without '*', $p \geq 0.05$ by unpaired t-test vs. the value without cerulenin treatment at the same time point.

We then identified the top ten abundant TAG species in the two strains during the 9 h sampling period and compared the concentration of these (Supplementary Fig. S3). The TAG species were grouped into either zero, one, two or three DHA-containing TAGs, designated TG(N/N/N), TG(N/N/22:6), TG(N/22:6/22:6) or TG(22:6/22:6/22:6), respectively, where N denotes any FA but DHA. From 3 to 12 h, the concentration of all groups increased in both T66 and SR21, except TG (22:6/22:6/22:6) in T66 (Fig. 5c and d).

The changes in the concentrations of TAG species in cerulenin-treated T66 had trends similar to those of SR21, but less significant (Fig. 5c and d). These results were in agreement with data obtained from the FA analyses. When considering the effect of FAS inhibition by cerulenin on the accumulation of DHA-containing TAGs, SR21 had higher TG(22:6/22:6/22:6) and TG(N/22:6/22:6), but lower TG(N/N/22:6) and TG(N/N/N) concentrations than the untreated cells after 3 h. From 3 to 12 h, TG(22:6/22:6/22:6) decreased more (T66) and increased less (SR21) in cerulenin-treated cells than the untreated cells, while TG(N/N/N) increased more in T66 (Fig. 5e and f). The result indicated that although the cerulenin-treated cells produced more DHA-rich TAG and fewer FAS-FA-rich TAGs in the first three hours, the different trends caused by cerulenin became less prominent after a longer cultivation period.

Table 1
Fatty acid production rate (g/l/h) of SR21 and T66 treated with cerulenin. FAS, the sum of C14:0, C16:0, C16:1 and C18:1; PKS, the sum of DHA and DPA. All data are expressed as mean ± the standard deviation of three independent cultures.

Time interval	Cerulenin (μM)	T66			SR21		
		FAS	DHA	PKS	FAS	DHA	PKS
0 h → 3 h	0	98 ± 5	46 ± 16	83 ± 25	213 ± 37	108 ± 36	152 ± 49
	1	95 ± 2	52 ± 11	96 ± 19	134 ± 26	100 ± 25	144 ± 32
	5	86 ± 41	71 ± 68	121 ± 94	68 ± 19	110 ± 34	160 ± 45
	25	74 ± 19	56 ± 28	100 ± 35	23 ± 21	115 ± 35	171 ± 49
3 h → 6 h	0	156 ± 105	94 ± 86	145 ± 120	224 ± 48	129 ± 31	169 ± 47
	1	143 ± 38	67 ± 28	105 ± 41	257 ± 42	177 ± 23	240 ± 35
	5	101 ± 89	51 ± 49	84 ± 75	233 ± 37	171 ± 17	226 ± 23
	25	105 ± 73	63 ± 49	107 ± 79	219 ± 9	129 ± 16	180 ± 24
6 h → 9 h	0	140 ± 47	28 ± 60	50 ± 80	313 ± 90	192 ± 50	261 ± 70
	1	116 ± 36	11 ± 15	19 ± 24	209 ± 44	151 ± 14	195 ± 17
	5	119 ± 26	-14 ± 32	-11 ± 43	234 ± 43	179 ± 40	241 ± 55
	25	124 ± 21	-30 ± 22	−37 ± 33	249 ± 27	223 ± 57	301 ± 82
9 h → 12 h	0	188 ± 9	16 ± 6	32 ± 7	270 ± 27	215 ± 24	284 ± 40
	1	239 ± 19	66 ± 23	113 ± 29	276 ± 74	198 ± 52	264 ± 69
	5	148 ± 83	26 ± 21	47 ± 36	286 ± 68	196 ± 45	263 ± 70
	25	156 ± 108	48 ± 62	75 ± 91	225 ± 73	154 ± 71	219 ± 91
0 h → 12 h	0	121 ± 24	34 ± 8	57 ± 13	202 ± 16	134 ± 12	178 ± 17
	1	125 ± 21	36 ± 14	59 ± 19	186 ± 18	131 ± 16	175 ± 23
	5	92 ± 30	16 ± 4	30 ± 7	188 ± 34	136 ± 25	182 ± 36
	25	96 ± 43	20 ± 22	36 ± 35	173 ± 26	127 ± 29	175 ± 38

3.5. The diacylglycerol and monoacylglycerol species of T66 and SR21 and how they were affected by cerulenin during N-starvation

Diacylglycerol (DAG) was the second most abundant lipid class in the two strains (Fig. 5a) and is one of the precursors for synthesizing other lipids, like TAG and phospholipids [22]. DG(16:1/22:6) and DG(18:1/22:6) were present in T66 (Fig. 6a). SR21 cannot produce C16:1 and C18:1 (Supplementary Fig. S1) [18], explaining their absence in this strain. DG(22:6/22:6), DG(16:0/16:0), DG(16:0/22:6), DG(14:0/22:6) are the possible DAG precursors to synthesize the top five abundant TAG species, TG(16:0/16:0/22:6), TG(16:0/22:6/22:6), TG(16:0/16:0/16:0), TG(14:0/16:0/22:6) and TG(22:6/22:6/22:6) (Supplementary Fig. S3). Interestingly, DG(22:6/22:6) was far more abundant than the other three in both strains (Fig. 6a). This was unexpected given that the concentration of DHA never was more than two times different to that of C16:0 (Supplementary Fig. S1).

The accumulation patterns for DAG and MAG were different for T66 and SR21. T66 contained a significantly higher proportion of DAG than SR21 after 3 h (Fig. 5a). From 3 to 12 h, the concentration of the most abundant species, DG(22:6/22:6) decreased in T66 but remained unchanged in SR21 (Fig. 6a). In the same period, the concentration of one DHA-containing DG species, designated DG(22:6/N), increased in T66 but remained unchanged in SR21 (Supplementary Fig. S4). From 3 to 12 h, MG(22:6) decreased in T66 but remained fairly constant in SR21

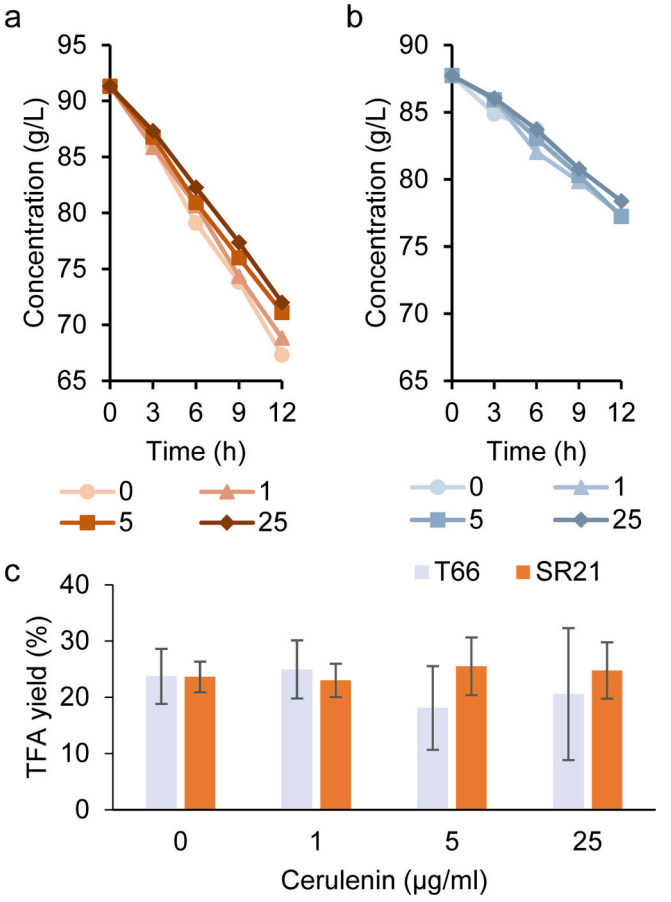

Fig. 3. Time-course profile for glucose consumption (glucose concentration left in the culture medium) of SR21 (a) and T66 (b) after treatment with cerulenin; (c) The yield of total fatty acids (TFA) on glucose for cerulenin-treated cells of SR21 and T66 after 12 h calculated as the proportion of glucose converted to TFA (weight %). The means of three independent cultures are shown, error bars represent the standard deviation.

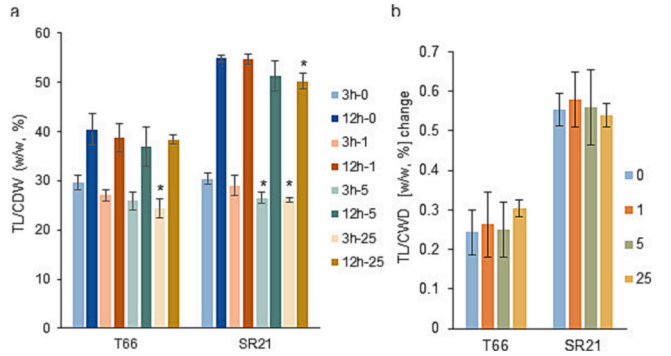

Fig. 4. The lipid content in T66 and SR21 after being treated with cerulenin for 3 and 12 h, displayed as the proportion of total lipids (TL) of cell dry weight (CDW) (a) and the difference of TL from 3 to 12 h (b). In the legends, 3 h and 12 h show time, while 0, 1, 5 and 25 show cerulenin concentrations (μM); All data are expressed as the mean of three independent cultures; Error bars represent the standard deviation. Data with '*', $p < 0.05$ by unpaired t-test vs. the value without cerulenin treatment at the same time point. Data without '*', $p \geq 0.05$ by unpaired t-test vs. the value without cerulenin treatment at the same time point.

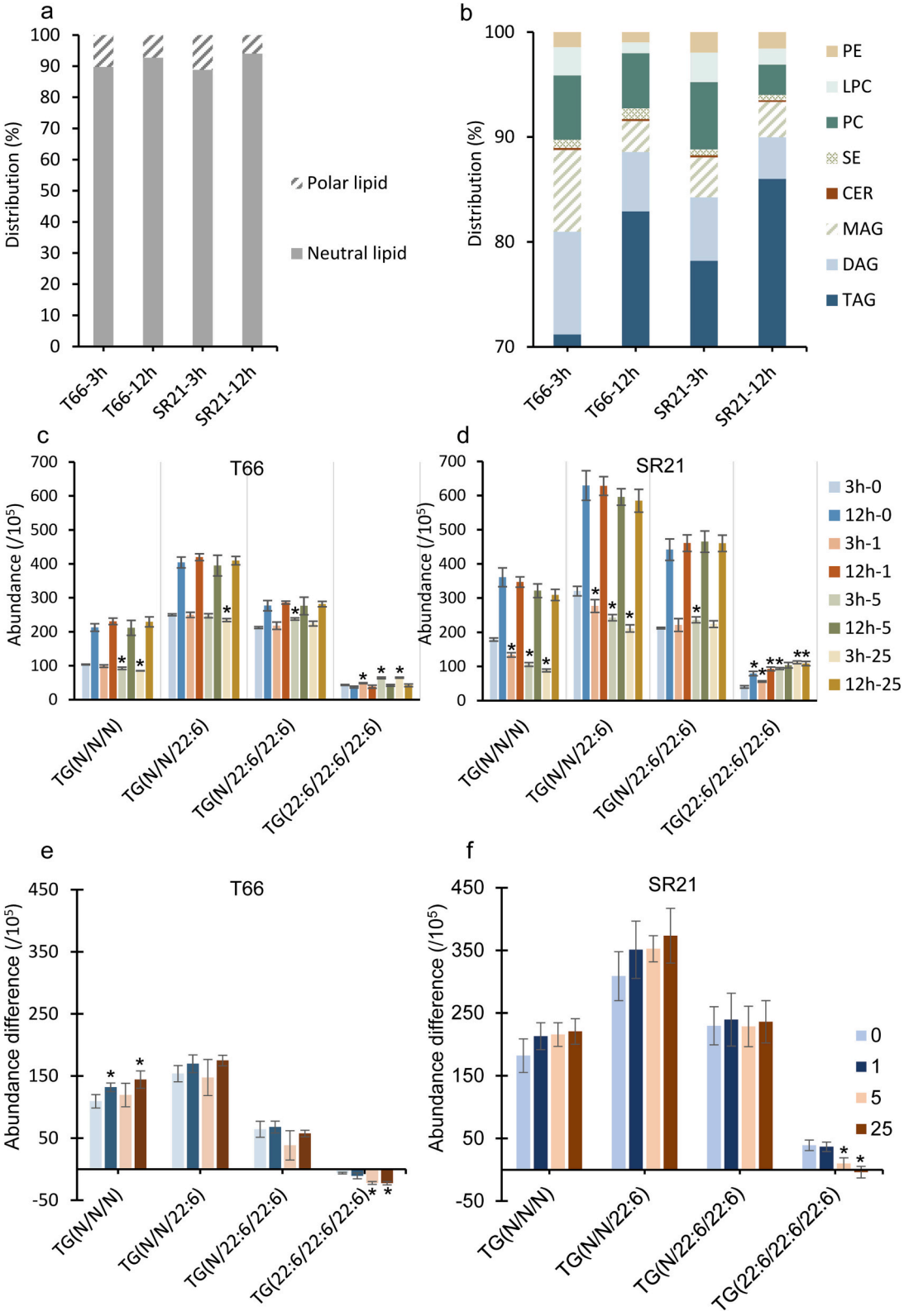

Fig. 5. The distribution between neutral lipid (TAG, DAG, MAG, CER and SE) and polar lipid (PC, LPC and PE) (a), and among lipid classes (b); Abundance of the top ten abundant TAG species (c); The abundance of TAG species grouped according to DHA content after being treated with cerulenin for 3 and 12 h in T66 (c) and SR21 (d), and the abundance difference from 3 to 12 h in T66 (c) and SR21 (f); In the legends, 3 h and 12 h show time, while 0, 1, 5 and 25 show cerulenin concentrations (μM). All data are expressed as the mean of three independent cultures; Error bars represent the standard deviation. TAG/TG, triacylglycerols; DAG, diacylglycerols; PC, phosphatidylcholines; MAG/MG, monoacylglycerols; LPC, lysophosphatidylcholines; PE, phosphatidylethanolamines; SE, steryl esters; CER, ceramides. All data are expressed as the mean of three independent cultures; Error bars represent the standard deviation. Data with '*', $p < 0.05$ by unpaired t-test vs. the value of the same lipid species without cerulenin treatment. Data without '*', $p \geq 0.05$ by unpaired t-test vs. the value of the same lipid species without cerulenin treatment.

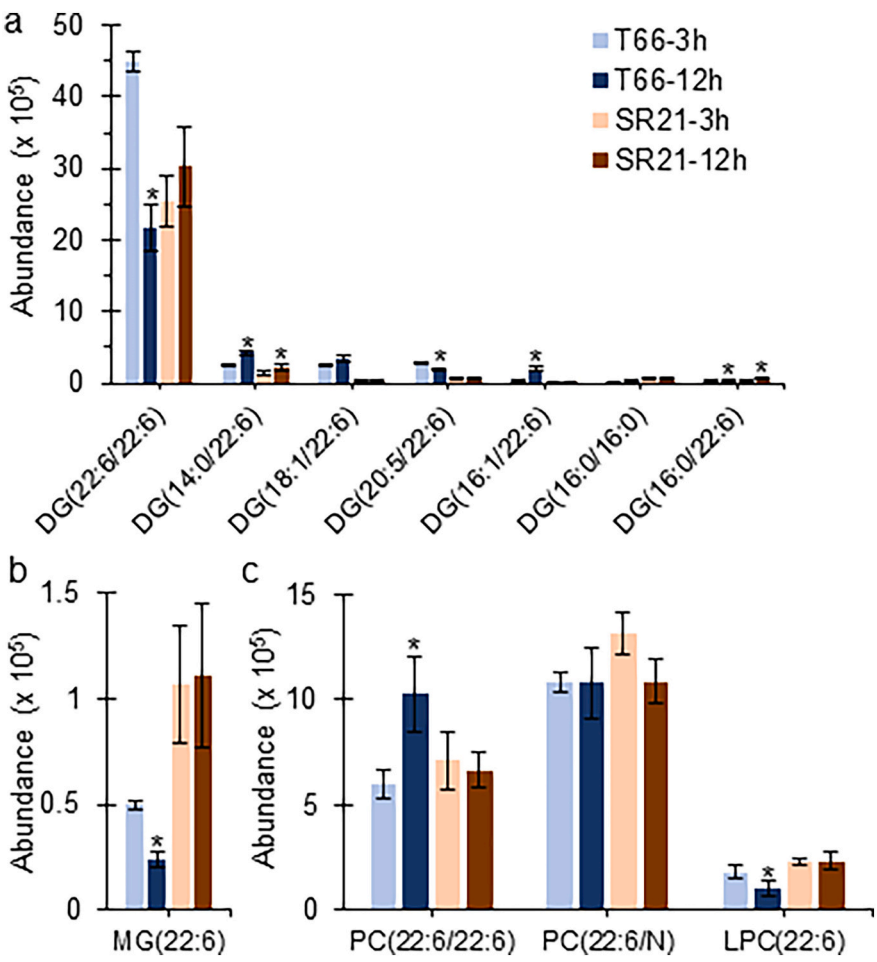

Fig. 6. The abundance of selected diacylglycerol (a), monoacylglycerol (b), phosphatidylcholine (PC) and lysophosphatidylcholine (LPC) (c) species in T66 and SR21 after entering N-starvation for 3 and 12 h. All data are expressed as the mean of three independent cultures; Error bars represent the standard deviation. Data with '*', $p < 0.05$ by unpaired t-test vs. the value of the same lipid species after entering N-starvation for 3 h. Data without '*', $p \geq 0.05$ by unpaired t-test vs. the value of the same lipid species after entering N-starvation for 3 h.

(Fig. 6b).

When FAS was inhibited by cerulenin, SR21, and to a mild extent, T66, had higher DG(22:6/22:6) concentrations than the untreated cells after 3 h. After 12 h, the difference in DG(22:6/22:6) concentrations between the cerulenin-treated and the untreated cells became insignificant (Supplementary Fig. S4). The result again indicated that the difference caused by cerulenin did not persist after a long period of N-starvation.

3.6. *The phospholipid species of T66 and SR21 and how they were affected by cerulenin during N-starvation*

Phosphatidylcholine (PC) was the most abundant phospholipid in both strains (Fig. 5a). PC can be the downstream product of DAG and the precursor of TAG [11,23]. When the accumulation of PC species in the two strains was compared, there were strain differences (Fig. 6c). PC (22:6/18:1) was present in T66, but not SR21, since SR21 cannot synthesize C18:1. PC species containing one DHA were grouped and designated PC(22:6/N). From 3 to 12 h, the PC(22:6/N) concentration remained unchanged in both strains, while PC(22:6/22:6) concentration increased in T66 but remained unchanged in SR21. DHA-containing lysophosphatidylcholine, LPC (22:6), can be generated from PC(22:6/22:6) [24]. From 3 to 12 h, LPC(22:6) concentration decreased in T66 but remained unchanged in SR21.

Cerulenin-treated SR21 and T66 had accumulated a similar level of different PC species to the untreated cells after 3 h. However, from 3 to 12 h, PC(22:6/22:6) decreased more in cerulenin-treated SR21 cells than in the untreated cells. This did, however, not occur in T66 (Supplementary Fig. S4).

4. Discussion

A main question in this study was whether a reduction of the consumption of the common precursors for PKS and FAS, such as acetyl-CoA and NADPH, by the FAS pathway, would enhance the production of the fatty acids produced by the PKS pathway. Earlier, thraustochytrid cells have been treated with cerulenin from the start of the fermentations, resulting in a higher proportion of DHA in the total FAs compared to untreated cells [12,13]. Growing (multiplying) cells contain phospholipids as the major lipid class [25]. In the present study, the aim was to study the TAG accumulation phase. The cells were therefore treated with cerulenin after N-exhaustion. Any result might be strain specific, and we chose to cultivate two different strains in parallel. Our results showed that cerulenin inhibited the FAS pathway in SR21, and in lesser extent, in T66, as the cerulenin-treated cells had a higher proportion of DHA of the total FAs than the untreated cells. However, there was no increase in the production rates of DHA. Furthermore, we recently demonstrated that in T66, the amount of lipid synthesis precursors, acetyl-CoA and NADPH increased after N-exhaustion, while the amount of long-chain fatty acyl-CoAs and lipid head group glycerol 3-P decreased [19]. Taken together, these results imply that for both strains the supplement of acetyl-CoA and NADPH is not limiting DHA synthesis, and that the rate-limiting step for DHA-synthesis must lay further down the pathway. The rate limiting step could for instance be the amount of the proteins comprising the DHA synthase complex or the acyl CoA synthetases that accept DHA as a substrate.

'DHA enrichment' in lipids during fermentation could reduce the cost of separation and purification in the following downstream process for producing high-DHA content lipid products in industry [15]. In this

study, the cerulenin-treated cells had higher concentrations of DHA-rich lipid species, TG(22:6/22:6/22:6), DG(22:6/22:6), and less FAS-rich TAG than untreated cells at the same time points (Fig. 5c, d and 6a). This is reasonable, due to a higher proportion of DHA in total FA, more DHA is available for the TAG synthesizing enzymes. This indicates a potential to enhance DHA-rich lipid production through strain engineering with a similar flux redistribution strategy.

The effect of cerulenin on FA synthesis was only seen at the first sampling point after three hours. The rates of FA synthesis were the same regardless of the amount of added cerulenin for the later time points. Similarly, the concentration differences of lipid species between the treated and untreated cells at 3 h, were reduced over the following nine hours, resulting in some of the differences becoming insignificant at 12 h. Earlier work has shown that organisms may inactivate cerulenin after some time, and this seems to be the case for the studied strains [26]. In addition, we have observed that T66 is more resistant to various antibiotics than SR21 (unpublished), and potentially to cerulenin as well, providing less significant results of the inhibitor in this strain.

Flux differences of enzyme reactions, caused by the amount of enzyme present and/or the enzyme properties, affect the accumulation of specific lipid species. In this study, DG(22:6/22:6) accumulated disproportionally higher in both T66 and SR21 during N-starvation compared to the other DAGs that can be the precursors for DHA-rich TAG. The result suggests that the conversion of DG(22:6/22:6) is a rate-limiting step in the production of DHA-rich TAG in *Aurantiochytrium* and related genera. This could potentially be overcome by strain engineering, such as identifying and overexpressing a DGAT or PDAT (Fig. 7) that prefer DG(22:6/22:6) as substrate. We also observed that the concentrations of some lipid species did not increase or decrease at the same time in the two strains in the absence of cerulenin, as summarized in Fig. 7. The DG(N/22:6) concentration increased in T66 but remained unchanged in SR21, while the concentration of MG(22:6), DG (22:6/22:6) and LPC(22:6) decreased in T66 but did not alter significantly in SR21. Moreover, the accumulation trends of TAG and PC species containing only DHA were different between the two strains, but both patterns have been observed for other thraustochytrid strains. The concentration of TG(22:6/22:6/22:6) increased but PC(22:6/22:6) remained unchanged in SR21, a similar pattern observed in *Schizochytrium* sp. A-2 before glucose exhaustion [27]. In contrast, TG(22:6/22:6/22:6) concentration remained unchanged but PC(22:6/22:6) concentration increased in T66, a trend that was observed in *Schizochytrium* sp. S31 before the exhaustion of glycerol [23]. DG is a potential common precursor of both TAG and PC (Fig. 7). Hence, the correlations suggest that reducing the CPT activity or increasing the PDAT activity in the lipid accumulation phase could be a way to enhance TG(22:6/22:6/22:6) synthesis.

Overall, this study shows that FAS inhibition increased the DHA proportion but not the DHA productivity in both strains, indicating that precursor availability for the PKS pathway is less likely to be the rate-limiting factor for DHA synthesis. FAS inhibition could also enrich DHA-rich TAG TG(22:6/22:6/22:6) production. However, since FAS synthesis is necessary for normal phospholipid membranes, one would then need to engineer the strain in order to avoid the increased expression of the FAS-encoding gene at the beginning of the lipid accumulation phase [20] Moreover, the conversion of DG(22:6/22:6) to TAGs is potentially a bottleneck for DHA-rich TAGs synthesis. These findings provide insights in thraustochytrid lipid metabolism that provides application potential in developing strains with improved DHA production.

Funding

This research was funded by Research Council of Norway, grant number 269432.

CRediT authorship contribution statement

E-Ming Rau: Conceptualization, Methodology, Investigation, Formal analysis, Validation, Writing – original draft, Writing – review & editing. **Inga Marie Aasen:** Conceptualization, Methodology, Investigation, Validation, Writing – review & editing. **Zdenka Bartosova:** Methodology, Investigation, Formal analysis, Validation, Writing – review & editing. **Per Bruheim:** Conceptualization, Methodology, Validation, Writing – review & editing. **Helga Ertesvåg:** Conceptualization,

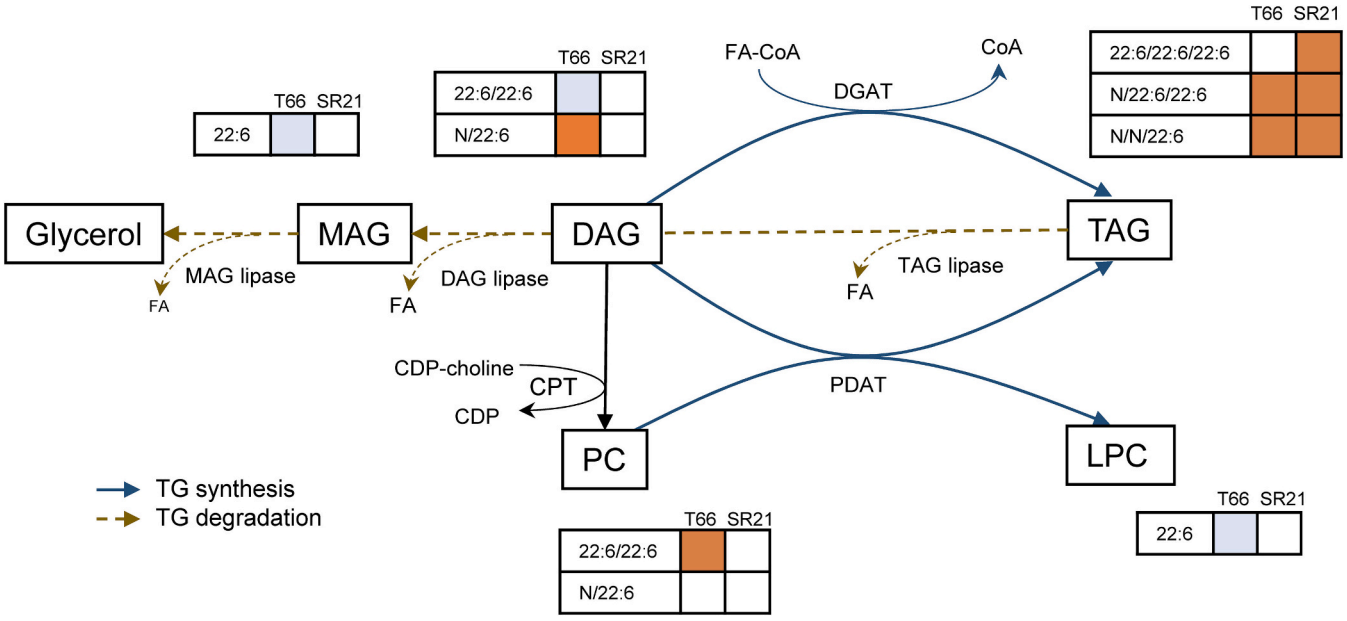

Fig. 7. Simplified lipid synthesis pathways in T66 and SR21, the abundance of DHA-containing lipid species either increased (orange), decreased (blue), or remained unchanged (white) under N-starvation from 3 to 12 h. TAG, triacylglycerol; DAG, diacylglycerol; MAG, monoacylglycerol; PC, phosphatidylcholine; LPC, lysophosphatidylcholine; DGAT, acyl-CoA:diacylglycerol acyltransferase; PDAT, phosphatidylcholine diacylglycerol choline phosphotransferase; CPT, CDP-choline: diacylglycerolcholine phosphotransferase; FA, fatty acid. (For interpretation of the references to colour in this figure legend, the reader is referred to the web version of this article.)

Methodology, Validation, Writing – review & editing.

Declaration of competing interest

The authors declare that they have no known competing financial interests or personal relationships that could have appeared to influence the work reported in this paper.

Data availability

Data will be made available on request.

Appendix A. Supplementary data

Supplementary data to this article can be found online at https://doi.org/10.1016/j.algal.2023.103091.

References

[1] M. Sprague, J.R. Dick, D.R. Tocher, Impact of sustainable feeds on omega-3 long-chain fatty acid levels in farmed Atlantic salmon, 2006–2015, Sci. Rep. 6 (2016) 21892, https://doi.org/10.1038/srep21892.

[2] C. Morabito, C. Bournaud, C. Maës, M. Schuler, R.Aiese Cigliano, Y. Dellero, E. Maréchal, A. Amato, F. Rébeillé, The lipid metabolism in thraustochytrids, Progr. Lipid Res 76 (2019) 101007, https://doi.org/10.1016/j.plipres.2019.101007.

[3] A. Patel, D. Karageorgou, E. Rova, P. Katapodis, U. Rova, P. Christakopoulos, L. Matsakas, An overview of potential oleaginous microorganisms and their role in biodiesel and omega-3 fatty acid-based industries, Microorganisms 8 (2020) 434, https://doi.org/10.3390/microorganisms8030434.

[4] I.M. Aasen, H. Ertesvåg, T.M.B. Heggeset, B. Liu, T. Brautaset, O. Vadstein, T. E. Ellingsen, Thraustochytrids as production organisms for docosahexaenoic acid (DHA), squalene, and carotenoids, Appl. Microbiol. Biotechnol. 100 (2016) 4309–4321, https://doi.org/10.1007/s00253-016-7498-4.

[5] X.M. Sun, Y.S. Xu, H. Huang, Thraustochytrid cell factories for producing lipid compounds, Trends Biotechnol. (2020), https://doi.org/10.1016/j.tibtech.2020.10.008.

[6] A. Hauvermale, J. Kuner, B. Rosenzweig, D. Guerra, S. Diltz, J.G. Metz, Fatty acid production in *Schizochytrium* sp.: involvement of a polyunsaturated fatty acid synthase and a type I fatty acid synthase, Lipids 41 (2006) 739–747, https://doi.org/10.1007/s11745-006-5025-6.

[7] Y. Ishibashi, H. Goda, R. Hamaguchi, K. Sakaguchi, T. Sekiguchi, Y. Ishiwata, Y. Okita, S. Mochinaga, S. Ikeuchi, T. Mizobuchi, Y. Takao, K. Mori, K. Tashiro, N. Okino, D. Honda, M. Hayashi, M. Ito, PUFA synthase-independent DHA synthesis pathway in *Parietichytrium* sp. and its modification to produce EPA and n-3DPA, Commun. Biol. 4 (2021) 1378, https://doi.org/10.1038/s42003-021-02857-w.

[8] J.W. Lee, D. Na, J.M. Park, J. Lee, S. Choi, S.Y. Lee, Systems metabolic engineering of microorganisms for natural and non-natural chemicals, Nat. Chem. Biol. 8 (2012) 536–546, https://doi.org/10.1038/nchembio.970.

[9] G. Lanéelle, A.K. Quémard, H. Marrakchi, InhA, a target of the antituberculous drug isoniazid, is involved in a mycobacterial fatty acid elongation system, FAS-II, Microbiol. 146 (2000) 289–296, https://doi.org/10.1099/00221287-146-2-289.

[10] B.H. Li, W.X. Tian, Inhibitory effects of flavonoids on animal fatty acid synthase, J. Biochem. 135 (2004) 85–91, https://doi.org/10.1093/jb/mvh010.

[11] X. Zhao, X. Qiu, Analysis of the biosynthetic process of fatty acids in *Thraustochytrium*, Biochimie 144 (2018) 108–114, https://doi.org/10.1016/j.biochi.2017.10.024.

[12] K.-C. Chaung, C.-Y. Chu, Y.-M. Su, Y.-M. Chen, Effect of culture conditions on growth, lipid content, and fatty acid composition of *Aurantiochytrium mangrovei* strain BL10, AMB Express 2 (2012) 42, https://doi.org/10.1186/2191-0855-2-42.

[13] W. Chen, P.P. Zhou, M. Zhang, Y.M. Zhu, X.P. Wang, X.A. Luo, Z.D. Bao, L.J. Yu, Transcriptome analysis reveals that up-regulation of the fatty acid synthase gene promotes the accumulation of docosahexaenoic acid in *Schizochytrium* sp S056 when glycerol is used, Algal Res. 15 (2016) 83–92, https://doi.org/10.1016/j.algal.2016.02.007.

[14] Y. Dellero, O. Cagnac, S. Rose, K. Seddiki, M. Cussac, C. Morabito, J. Lupette, R. A. Cigliano, W. Sanseverino, M. Kuntz, J. Jouhet, E. Marechal, F. Rebeille, A. Amato, Proposal of a new thraustochytrid genus *Hondaea* gen. Nov and comparison of its lipid dynamics with the closely related pseudo-cryptic genus *Aurantiochytrium*, Algal Res. 35 (2018) 125–141, https://doi.org/10.1016/j.algal.2018.08.018.

[15] G. Chang, Z. Luo, S. Gu, Q. Wu, M. Chang, X. Wang, Fatty acid shifts and metabolic activity changes of *Schizochytrium* sp. S31 cultured on glycerol, Bioresour. Technol. 142 (2013) 255–260, https://doi.org/10.1016/j.biortech.2013.05.030.

[16] A.N. Jakobsen, I.M. Aasen, K.D. Josefsen, A.R. Strøm, Accumulation of docosahexaenoic acid-rich lipid in thraustochytrid *Aurantiochytrium* sp. strain T66: effects of N and P starvation and O2 limitation, Appl. Microbiol. Biotechnol. 80 (2008) 297–306, https://doi.org/10.1007/s00253-008-1537-8.

[17] T. Yokochi, D. Honda, T. Higashihara, T. Nakahara, Optimization of docosahexaenoic acid production by *Schizochytrium limacinum* SR21, Appl. Microbiol. Biotechnol. 49 (1998) 72–76, https://doi.org/10.1007/s002530051139.

[18] E.M. Rau, I.M. Aasen, H. Ertesvåg, A non-canonical Δ9-desaturase synthesizing palmitoleic acid identified in the thraustochytrid *Aurantiochytrium* sp. T66, Appl. Microbiol. Biotechnol. (2021), https://doi.org/10.1007/s00253-021-11425-5.

[19] Z. Bartosova, H. Ertesvåg, E.L. Nyfløt, K. Kämpe, I.M. Aasen, P. Bruheim, Combined metabolome and lipidome analyses for in-depth characterization of lipid accumulation in the DHA producing *Aurantiochytrium* sp, T66, Metabolites 11 (2021), https://doi.org/10.3390/metabo11030135.

[20] T.M.B. Heggeset, H. Ertesvåg, B. Liu, T.E. Ellingsen, O. Vadstein, I.M. Aasen, Lipid and DHA-production in *Aurantiochytrium* sp. – responses to nitrogen starvation and oxygen limitation revealed by analyses of production kinetics and global transcriptomes, Sci. Rep. 9 (2019) 19470, https://doi.org/10.1038/s41598-019-55902-4.

[21] Z. Bartosova, S.V. Gonzalez, A. Voigt, P. Bruheim, High throughput semiquantitative UHPSFC-MS/MS lipid profiling and lipid class determination, J. Chromatogr. Sci. 59 (2021) 670–680, https://doi.org/10.1093/chromsci/bmaa121.

[22] T. Furmanek, K. Demski, W. Banaś, R. Haslam, J. Napier, S. Stymne, A. Banaś, The utilization of the acyl-CoA and the involvement PDAT and DGAT in the biosynthesis of erucic acid-rich triacylglycerols in crambe seed oil, Lipids 49 (2014) 327–333, https://doi.org/10.1007/s11745-014-3886-7.

[23] M. Chang, T. Zhang, L. Li, F. Lou, M. Ma, R. Liu, Q. Jin, X. Wang, Choreography of multiple omics reveals the mechanism of lipid turnover in *Schizochytrium* sp. S31, Algal Res 54 (2021) 102182, https://doi.org/10.1016/j.algal.2021.102182.

[24] A. Dahlqvist, U. Ståhl, M. Lenman, A. Banas, M. Lee, L. Sandager, H. Ronne, S. Stymne, Phospholipid:diacylglycerol acyltransferase: an enzyme that catalyzes the acyl-CoA-independent formation of triacylglycerol in yeast and plants, Proc. Natl. Acad. Sci. U. S. A. 97 (2000) 6487–6492, https://doi.org/10.1073/pnas.120067297.

[25] L.-J. Ren, G.-N. Sun, X.-J. Ji, X.-C. Hu, H. Huang, Compositional shift in lipid fractions during lipid accumulation and turnover in *Schizochytrium* sp, Bioresour. Technol. 157 (2014) 107–113, https://doi.org/10.1016/j.biortech.2014.01.078.

[26] H. Takeshima, C. Kitao, S. Omura, Inhibition of the biosynthesis of leucomycin, a macrolide antibiotic, by cerulenin, J. Biochem. 81 (1977) 1127–1132, https://doi.org/10.1093/oxfordjournals.jbchem.a131537.

[27] X.-H. Yue, W.-C. Chen, Z.-M. Wang, P.-Y. Liu, X.-Y. Li, C.-B. Lin, S.-H. Lu, F.-H. Huang, X. Wan, Lipid distribution pattern and transcriptomic insights revealed the potential mechanism of docosahexaenoic acid traffics in *Schizochytrium* sp. A-2, J. Agr. Food Chem. 67 (2019) 9683–9693, https://doi.org/10.1021/acs.jafc.9b03536.